

RESEARCH OUTPUTS / RÉSULTATS DE RECHERCHE

A class of trust region methods for nonlinear network optimization problems

Sartenaer, Annick

Published in:
SIAM Journal on Optimization

Publication date:
1995

Document Version
Peer reviewed version

[Link to publication](#)

Citation for pulished version (HARVARD):
Sartenaer, A 1995, 'A class of trust region methods for nonlinear network optimization problems', *SIAM Journal on Optimization*, vol. 5, no. 2, pp. 379-407.

General rights

Copyright and moral rights for the publications made accessible in the public portal are retained by the authors and/or other copyright owners and it is a condition of accessing publications that users recognise and abide by the legal requirements associated with these rights.

- Users may download and print one copy of any publication from the public portal for the purpose of private study or research.
- You may not further distribute the material or use it for any profit-making activity or commercial gain
- You may freely distribute the URL identifying the publication in the public portal ?

Take down policy

If you believe that this document breaches copyright please contact us providing details, and we will remove access to the work immediately and investigate your claim.

A CLASS OF TRUST REGION METHODS FOR NONLINEAR NETWORK OPTIMIZATION PROBLEMS

A. SARTENAER*

Abstract. We describe the results of a series of tests upon a class of new methods of trust region type for solving the nonlinear network optimization problem. The trust region technique considered is characterized by the use of the infinity norm and of inexact projections on the network constraints. The results are encouraging and show that this approach is particularly useful in solving large-scale nonlinear network optimization problems, especially when many bound constraints are expected to be active at the solution.

Key Words. Nonlinear optimization, nonlinear network optimization, trust region methods, truncated Newton methods, numerical results

1. Introduction. We consider the problem:

$$(1.1) \quad \begin{array}{ll} \min_{x \in \mathbf{R}^n} & f(x) \\ \text{subject to} & Ax = b \\ & l \leq x \leq u, \end{array}$$

where $f : \mathbf{R}^n \rightarrow \mathbf{R}$ is a twice continuously differentiable partially separable function, A is a $m \times n$ node-arc incidence matrix, $b \in \mathbf{R}^m$ and satisfies $\sum_{i=1}^m b_i = 0$, and l and $u \in \mathbf{R}^n$.

Many algorithms for solving the nonlinear network problem (1.1) have been proposed (see [1], [3], [10], [11], [13], [21] and [22] for instance), most of them being of the active set variety. In particular, a sequence of problems are solved for which a subset of the variables (the active set) are fixed at bounds and the objective function is minimized with respect to the remaining variables. Such algorithms typically use linesearches to enforce convergence. A significant drawback of these methods, especially for large-scale problems, is that the active sets are allowed to change slowly and many iterations are necessary to correct a bad initial choice.

In this paper, we propose a new algorithm of *trust region* type that allows rapid changes in the active set. This algorithm is an adaptation of the one proposed by Conn, Gould, Sartenaer and Toint in [4] for which we have already produced a general convergence theory. At iteration k of the algorithm, we define a local model of the objective function at the current iterate, x_k say, and a *region* surrounding x_k where we *trust* this model. The algorithm then finds, in this region, a candidate for the next iterate that sufficiently reduces the value of the model. If the function value calculated at this point matches its predicted value closely enough, then the new point is accepted as the next iterate and the trust region is possibly enlarged. Otherwise, the point is rejected and the trust region size is decreased.

The determination of a candidate for the next iterate requires the computation of a *Generalized Cauchy Point* which expands the notion of a Cauchy Point to problems with general convex constraints (see [4]). This has the double advantage of allowing significant changes in the active set at each iteration and permitting the extension of well-known convergence results for trust region methods applied to unconstrained problems (see [18]) and to simple bound constrained problems (see [7]).

* Department of Mathematics, Facultés Universitaires ND de la Paix, 61 rue de Bruxelles, B-5000, Namur, Belgium.

The calculation of a suitable Generalized Cauchy Point, which makes use of the first order information, is performed by solving a sequence of *linear network* problems. The Generalized Cauchy Point is thereafter refined to calculate a candidate for the next iterate using the second order information through a *truncated conjugate gradient* technique. This technique, as well as the linear solver used for the Generalized Cauchy Point, takes advantage of the network structure in the constraints of problem (1.1) by combining a data structure of the type proposed by Bradley, Brown and Graves [2] with a partition of the variables similar to that proposed by Murtagh and Saunders [19] implemented in MINOS, also making use of *variable reduction matrices*. Moreover, we use the concept of *maximal basis* that is especially well suited in our context to allow adequate adaptation of the theory developed in [4] for the active set identification strategy. Note that most of the aforementioned techniques are equally exploited in successful existing large-scale nonlinear network solvers, such as GENOS [1] and NLPNET [10].

Section 2 of the paper gives a general introduction to the framework of our algorithm, together with a detailed description of the computation of a Generalized Cauchy Point and of a candidate for the next iterate. The optimality conditions and the specific algorithm are also presented in this section. Section 3 reports and comments on some numerical experiments, and includes a comparison with an existing available specialized software for the same problem. Finally some conclusions and perspectives are outlined in §4.

2. Description of the algorithm.

2.1. The basic algorithm. As already mentioned, our algorithm is of trust region type and the description given here is a special case of the general framework presented in [4], adapted to the solution of problem (1.1). We first introduce the following concepts. The *feasible region* for problem (1.1) is the polyhedral set

$$X = \{x \in \mathbf{R}^n \mid Ax = b \text{ and } l \leq x \leq u\},$$

and any point x in the feasible region is called *feasible*. We define the *active set with respect to the vectors l and u at the feasible point x* as the index set

$$\mathcal{A}(x, l, u) = \{i \in \{1, \dots, n\} \mid [x]_i = [l]_i \text{ or } [x]_i = [u]_i\},$$

where $[v]_i$ denotes the i th component of the vector v .

At the k th stage of the algorithm, we suppose that we have a feasible point x_k , the exact gradient $\nabla f(x_k)$ (denoted g_k) and the exact Hessian $\nabla^2 f(x_k)$ (denoted H_k) of the objective function at x_k . We also require a scalar $\Delta_k > 0$ for the trust region radius, and choose the quadratic model of the form

$$m_k(x_k + s) \stackrel{\text{def}}{=} f(x_k) + g_k^T s + \frac{1}{2} s^T H_k s$$

to approximate the objective function around x_k . A trial feasible step s_k is then computed by approximately solving the trust region problem

$$(2.1) \quad \begin{array}{ll} \min_{s \in \mathbf{R}^n} & m_k(x_k + s) \\ \text{subject to} & As = 0 \\ & l \leq x_k + s \leq u \\ \text{and} & \|s\| \leq \Delta_k, \end{array}$$

where $\|\cdot\|$ is a suitable chosen norm. The updates of the iterate x_k and of Δ_k are done using the same criteria of acceptance as in trust region methods for unconstrained or bound constrained minimization (see [18] and [7]). That is,

$$x_{k+1} = \begin{cases} x_k + s_k & \text{if } \rho_k > \eta_1 \\ x_k & \text{if } \rho_k \leq \eta_1 \end{cases}$$

and

$$(2.2) \quad \Delta_{k+1} = \begin{cases} 2\Delta_k & \text{if } \rho_k \geq \eta_2 \\ \Delta_k & \text{if } \eta_1 < \rho_k < \eta_2 \\ \frac{1}{2} \min(\|s_k\|, \Delta_k) & \text{if } \rho_k \leq \eta_1, \end{cases}$$

where

$$\rho_k = \frac{f(x_k) - f(x_k + s_k)}{m_k(x_k) - m_k(x_k + s_k)}$$

represents the ratio of the achieved to the predicted reduction of the objective function and $0 < \eta_1 < \eta_2 < 1$ are appropriate numbers. It now remains to describe our approximate solution of (2.1).

The choice of the infinity norm for the trust region constraint in problem (2.1) allows us to replace the bound constraints and the trust region constraint in this problem by the bound constraints

$$(2.3) \quad \max([l]_i, [x_k]_i - \Delta_k) \stackrel{\text{def}}{=} [l_k]_i \leq [x_k + s]_i \leq [u_k]_i \stackrel{\text{def}}{=} \min([u]_i, [x_k]_i + \Delta_k)$$

for $i = 1, \dots, n$. Problem (2.1) then becomes

$$(2.4) \quad \begin{array}{ll} \min_{s \in \mathbf{R}^n} & m_k(x_k + s) \\ \text{subject to} & As = 0 \\ & l_k \leq x_k + s \leq u_k. \end{array}$$

In order to satisfy the global convergence theory developed in [4], we need to find a feasible point $x_k + s_k$ within the trust region at which the value of the model function is no larger than its value at the Generalized Cauchy Point (GCP). This GCP, denoted x_k^C , is found through a *projected search* on the model along an *approximation* of the projected gradient path (i.e. the projection of the gradient on the feasible set). Note that the determination of the active set (the set of variables that are to be fixed at one of their bounds during the current iteration) takes place when finding the GCP. Since no restriction on the number of variables moving in or out the active set is imposed from one iteration to the other, rapid changes may occur in the active set. This is extremely useful in large-scale optimization problems since the number of iterations required to find the correct active set may hence be considerably smaller than the number of active bounds at the solution. Subsequently we use second order information to refine the GCP and provide a fast ultimate rate of convergence. Therefore, following Murtagh and Saunders [19], we first partition the matrix A as

$$A = (B \quad S \quad N)$$

where the $m \times m$ submatrix B is nonsingular, and define

$$(2.5) \quad \{1, \dots, n\} = \mathcal{B} \cup \mathcal{S} \cup \mathcal{N},$$

the induced partition of the variable indices. For a node-arc incidence matrix, Dantzig [9, p. 356] has shown that the arcs whose indices are in \mathcal{B} form a *spanning tree* of the network. (These arcs are called *basic arcs* while the arcs whose indices are in \mathcal{S} and \mathcal{N} are called *superbasic arcs* and *nonbasic arcs* respectively.) In that case, it is worth using a specialized data structure of the type proposed by Bradley, Brown and Graves [2] that allows us to store and update the basis of the network (i.e. the spanning tree) in a very efficient manner.

According to assumption (AS.8) in [4],

$$(2.6) \quad \mathcal{A}(x_k^C, l, u) \subseteq \mathcal{A}(x_k + s_k, l, u)$$

— the variables of x_k^C that are at a bound must remain fixed when finding a better approximation of a minimizer of (2.4). We then set, at each iteration k ,

$$(2.7) \quad \mathcal{N} = \mathcal{A}(x_k^C, l_k, u_k) \setminus \mathcal{B} \quad \text{and} \quad \mathcal{S} = \{1, \dots, n\} \setminus (\mathcal{B} \cup \mathcal{N}).$$

Since $j \notin \mathcal{A}(x_k^C, l_k, u_k) \implies j \notin \mathcal{A}(x_k^C, l, u)$, this choice for \mathcal{N} produces a correct set for \mathcal{S} according to assumption (2.6), namely an index set of arcs $\notin \mathcal{B}$ strictly between the bounds l and u . Note that this choice imposes more than the assumption requires, since it further fixes the components of the GCP that are on the trust region boundary (even if they are not at a bound l or u), which seems quite natural.

Using a *variable reduction matrix* Z as proposed by Murtagh and Saunders [19] (that is a matrix formed by column vectors that belong to the nullspace of A , yielding the relation $AZ = 0$) and choosing

$$(2.8) \quad Z = \begin{pmatrix} -B^{-1}S \\ I \\ 0 \end{pmatrix},$$

we then solve approximately problem (2.4) by applying a conjugate gradient algorithm, starting from the GCP, to the equation

$$Z^T H_k Z [s]_{\mathcal{S}} = -Z^T g_k.$$

Let $[s_k]_{\mathcal{S}}$ be the approximation found. We define the full trial step s_k by $s_k = ([s_k]_{\mathcal{B}}, [s_k]_{\mathcal{S}}, [s_k]_{\mathcal{N}})$ where $[s_k]_{\mathcal{B}}$ and $[s_k]_{\mathcal{N}}$ satisfy

$$(2.9) \quad B [s_k]_{\mathcal{B}} = -S [s_k]_{\mathcal{S}}$$

and

$$[s_k]_{\mathcal{N}} = 0.$$

We defer to §2.3 the management of the constraints $l_k \leq x_k + s \leq u_k$ during the conjugate gradient schemes solving problem (2.4). Note that the matrix Z in (2.8) exhibits a useful structure [16]. Indeed, the j th column of Z corresponds to the cycle formed by adding the j th superbasic arc to the spanning tree associated with the basis. This cycle can be decomposed in the j th superbasic arc, joining nodes e and f , say, and its associated *flow augmenting path* (also called *basic equivalent path*), which is the (unique) path between nodes e and f belonging to the tree. Let β_j be the set

of indices of the arcs of this path. The element (i, j) of $-B^{-1}S$ is then given by

$$(2.10) \quad [-B^{-1}S]_{ij} = \begin{cases} +1 & \text{if } i \in \beta_j \text{ and the } i\text{th basic arc has an orientation identical to that of the } j\text{th superbasic arc in the cycle,} \\ -1 & \text{if } i \in \beta_j \text{ and the } i\text{th basic arc has an orientation opposite to that of the } j\text{th superbasic arc in the cycle,} \\ 0 & \text{if } i \notin \beta_j. \end{cases}$$

This special structure allows for a compact storage of the matrix Z , as well as for very efficient techniques for computing products that involve this matrix or its transpose (see [22] for more details). Moreover, this last structure is analogous to that of the matrix $-B^{-1}N$ that arises in the computation of the Lagrange multiplier estimates,

$$[g_k]_{\mathcal{N}} - N^T B^{-T} [g_k]_{\mathcal{B}},$$

with the only difference being that the flow augmenting path is now associated with a nonbasic variable instead of a superbasic one.

In order to be sure that assumption (2.6) holds, we further need to impose that the basic arcs whose indices are in $\mathcal{A}(x_k^C, l, u)$ remain fixed when finding the candidate step s_k . But this can be automatically induced by using the concept of *maximal spanning tree*, as introduced by Dembo and Klincewicz in [12], that is a spanning tree which has a maximal number of arcs whose flows are strictly between the bounds l and u (see also [23]). With such a spanning tree, a basic arc whose flow is at a bound is not allowed to belong to the flow augmenting path of a *free* arc (that is an arc whose flow is strictly between its bounds), since otherwise, the replacement of this basic arc with the free one would increase the number of free arcs in the spanning tree, in contradiction with its property of maximality. Given the way the index sets \mathcal{N} and \mathcal{S} are defined in (2.7), every superbasic arc is ensured to be strictly between the bounds l and u , and the use of maximal spanning trees therefore prevents any basic arc that belongs to the flow augmenting path of a superbasic arc to be at one of its bounds. Consequently, since a basic component of s_k computed from (2.9) may be non-zero *only if* its corresponding arc belongs to the flow augmenting path of at least one superbasic arc (see (2.10)), we are sure that the only basic arcs allowed to change during the process are those which are strictly between the bounds l and u . Moreover, using the same argument, we force the basic arcs that are on the trust region boundary to remain fixed by imposing that the spanning tree be maximal *also with respect* to the bounds l_k and u_k (that is to have a maximal number of arcs whose flows are strictly between the bounds l_k and u_k).

Under condition (2.6) and a nondegeneracy condition, the strategy described above is sufficient to ensure that the correct active set is identified after a finite number of iterations (see [4]). We now give, in the next two sections, more details on the computations of the GCP x_k^C and the trial step s_k .

2.2. The Generalized Cauchy Point. Following [4], in order to find a Generalized Cauchy Point, we first need to determine an approximation of a suitable point on the projected gradient path. By this, we mean a feasible point $x_k^C = x_k + s_k^C$ inside the trust region that satisfies the inequality

$$(2.11) \quad g_k^T s_k^C \leq -\mu_3 \alpha_k(t_k)$$

for some fixed $\mu_3 \in (0, 1]$ and $t_k > 0$. Here $\alpha_k(t_k) > 0$ represents the magnitude of the maximum decrease of the linearized model achievable on the intersection of the feasible domain with a box of radius t_k centered at x_k :

$$(2.12) \quad -\alpha_k(t_k) \stackrel{\text{def}}{=} \min_{d \in \mathbf{R}^n} \quad g_k^T d \\ \text{subject to} \quad Ad = 0 \\ l_{t_k} \leq d \leq u_{t_k},$$

where

$$[l_{t_k}]_j \stackrel{\text{def}}{=} \max([l]_j, [x_k]_j - t_k) - [x_k]_j$$

and

$$[u_{t_k}]_j \stackrel{\text{def}}{=} \min([u]_j, [x_k]_j + t_k) - [x_k]_j$$

for $j = 1, \dots, n$. Furthermore, this point must satisfy the two Goldstein-like conditions

$$(2.13) \quad m_k(x_k + s_k^C) \leq m_k(x_k) + \mu_1 g_k^T s_k^C$$

and

$$(2.14) \quad \text{either } t_k \geq \min[\nu_1 \Delta_k, \nu_2] \text{ or } m_k(x_k + s_k^C) \geq m_k(x_k) + \mu_2 g_k^T s_k^C,$$

where $0 < \mu_1 < \mu_2 < 1$, $\nu_1 \in (0, 1)$ and $\nu_2 \in (0, 1]$ are appropriate constants.

The *GCP Algorithm* given in [4] is a model algorithm for computing a Generalized Cauchy Point that verifies conditions (2.11), (2.13) and (2.14). It is iterative and uses bisection. At each iteration i , given a bisection parameter value $t_i > 0$, it computes first a candidate step s_i that satisfies condition (2.11) (with $t_k = t_i$ and $s_k^C = s_i$), checking then conditions (2.13) and (2.14) (with $t_k = t_i$ and $s_k^C = s_i$), until either an acceptable GCP is found or two candidates $x_k + s_k^l$ and $x_k + s_k^u$ are known that violate condition (2.13) and condition (2.14). Thus, if an acceptable GCP is not yet found, the algorithm carries out a simple bisection linesearch on the model along a particular path between these two points, yielding a suitable GCP in a finite number of iterations. This particular path, called the *restricted path*, is obtained by applying the so-called *restriction operator*,

$$R_{x_k}[y] \stackrel{\text{def}}{=} \arg \min_{z \in [x_k, y] \cap X} \|z - y\|_2$$

where $[x_k, y]$ is the segment between x_k and y , on the piecewise linear path consisting of the segment $[x_k + s_k^l, x_k + s_k^p]$ followed by $[x_k + s_k^p, x_k + s_k^u]$, where

$$s_k^p = \max \left[1, \frac{\|s_k^u\|_\infty}{\|s_k^l\|_\infty} \right] s_k^l.$$

This restricted path is an approximation of the unknown projected gradient path between the points $x_k + s_k^l$ and $x_k + s_k^u$ in the sense that each point on this path satisfies condition (2.11) for some $t_k > 0$. It also closely follows the boundary of the feasible domain, as does the projected gradient path. We refer the reader to [4] for a detailed discussion of these concepts.

In order to perform the simple bisection linesearch along the restricted path, a call to the *RS Algorithm* given below is made in the GCP Algorithm. The inner iterations of Algorithm RS are denoted by the index j .

RS Algorithm.

Step 0. Initialization. Set $\delta_p = \|s_k^p - s_k^l\|_2$, $\delta_u = \delta_p + \|s_k^u - s_k^p\|_2$, $l_0 = 0$, $u_0 = \delta_u$ and $j = 0$. Then define $\delta_0 = \frac{1}{2}(l_0 + u_0)$.

Step 1. Compute the point on the restricted path corresponding to δ_j .

Step 1.0. Compute the step from x_k to the piecewise linear path. Set

$$s_j \stackrel{\text{def}}{=} \begin{cases} \frac{\delta_j}{\delta_p} s_k^p + (1 - \frac{\delta_j}{\delta_p}) s_k^l & \text{if } \delta_j \leq \delta_p, \\ \frac{\delta_j - \delta_p}{\delta_u - \delta_p} s_k^u + (1 - \frac{\delta_j - \delta_p}{\delta_u - \delta_p}) s_k^p & \text{if } \delta_j \geq \delta_p. \end{cases}$$

Step 1.1. Calculate the smallest value of α such that $x_k + \alpha s_j$ hits a bound. Set

$$\alpha^* = \min \left[\min_{\{i \in \{1, \dots, n\} | [s_j]_i < 0\}} \left| \frac{[x_k]_i - [l]_i}{[s_j]_i} \right|, \min_{\{i \in \{1, \dots, n\} | [s_j]_i > 0\}} \left| \frac{[x_k]_i - [u]_i}{[s_j]_i} \right| \right].$$

Step 1.2. Compute the point on the restricted path. Set

$$\alpha_j = \min[1, \alpha^*]$$

and

$$x_j = x_k + \alpha_j s_j.$$

Step 2. Check the stopping conditions. If

$$(2.15) \quad m_k(x_j) > m_k(x_k) + \mu_1 g_k^T(x_j - x_k),$$

then set

$$l_{j+1} = l_j \quad \text{and} \quad u_{j+1} = \delta_j,$$

and go to Step 3. Else, if

$$(2.16) \quad m_k(x_j) < m_k(x_k) + \mu_2 g_k^T(x_j - x_k),$$

then set

$$l_{j+1} = \delta_j \quad \text{and} \quad u_{j+1} = u_j,$$

and go to Step 3; else (that is if both (2.15) and (2.16) fail), set $x_k^C = x_j$ and STOP.

Step 3. Choose the next parameter value by bisection. Increment j by one, set

$$\delta_j = \frac{1}{2}(l_j + u_j)$$

and go to Step 1.

Note that the point x_j calculated at Step 1 satisfies the constraint $Ax = b$ and minimizes the distance from $x_k + s_j$ in the direction $-s_j$ while satisfying the constraints $l \leq x_j \leq u$, as expected.

As mentioned before, at a given iteration i of the GCP Algorithm we first compute a candidate step s_i that satisfies condition

$$(2.17) \quad g_k^T s_i \leq -\mu_3 \alpha_k(t_i)$$

where t_i is the current bisection parameter value. We obtain s_i by applying a simplex-like algorithm to problem (2.12) (where t_k is replaced by t_i) and by stopping this algorithm as soon as an admissible iterate d_ℓ has been found that verifies

$$(2.18) \quad |g_k^T d_\ell| \geq \mu_3 \min_{r=1, \dots, \ell} [l_{t_i}^T A^T \pi_r + (u_{t_i} - l_{t_i})^T \mu_r - g_k^T l_{t_i}],$$

where

$$(2.19) \quad \pi_r = [g_k]_{\mathcal{B}_r}^T B_r^{-1} \text{ and } [\mu_r]_j = \max(0, \pi_r A e_j - [g_k]_j) \quad (j = 1, \dots, n),$$

where B_r is the admissible basis associated with some previous candidate d_r , $[g_k]_{\mathcal{B}_r}$ is the basic part of g_k and e_j is the j -th vector of the canonical basis of \mathbf{R}^n . Indeed, the right-hand-side of condition (2.18) is an upper bound on the value of $\mu_3 \alpha_k(t_i)$ and (2.18) thus implies condition (2.17) for $s_i = d_\ell$ (see [4] for more details).

Now we give the GCP Algorithm itself. Its inner iterations are denoted by the index i .

GCP Algorithm.

Step 0. Initialization. Choose $\lambda \in (0, 1)$. Set $l_0 = 0$, $u_0 = \Delta_k$, $s_0^l = 0$ and $i = 0$. Also choose s_0^u an arbitrary vector such that $\|s_0^u\|_\infty > \Delta_k$ and an initial parameter $t_0 \in (0, \Delta_k]$.

Step 1. Compute a candidate step. Compute a vector s_i such that

$$A s_i = 0 \text{ and } l_{t_i} \leq s_i \leq u_{t_i},$$

and

$$g_k^T s_i \leq -\mu_3 \alpha_k(t_i).$$

Step 2. Check the stopping rules on the model and step. If

$$(2.20) \quad m_k(x_k + s_i) > m_k(x_k) + \mu_1 g_k^T s_i,$$

then set

$$u_{i+1} = t_i \quad s_{i+1}^u = s_i$$

and

$$l_{i+1} = l_i \quad s_{i+1}^l = s_i^l,$$

and go to Step 3. Else, if

$$(2.21) \quad m_k(x_k + s_i) < m_k(x_k) + \mu_2 g_k^T s_i$$

and

$$(2.22) \quad t_i < \min[\nu_1 \Delta_k, \nu_2],$$

then set

$$u_{i+1} = u_i \quad s_{i+1}^u = s_i^u$$

and

$$l_{i+1} = t_i \quad s_{i+1}^l = s_i,$$

and go to Step 3. Else (that is if (2.20) and either (2.21) or (2.22) fail), then set

$$x_k^C = x_k + s_i$$

and STOP.

Step 3. Define a new trial step by bisection. We distinguish two mutually exclusive cases.

Case 1. $s_{i+1}^l = s_0^l$ or $s_{i+1}^u = s_0^u$. Set

$$t_{i+1} = \lambda(l_{i+1} + u_{i+1}),$$

increment i by one and go to Step 1.

Case 2. $s_{i+1}^l \neq s_0^l$ and $s_{i+1}^u \neq s_0^u$. Set

$$s_k^l = s_{i+1}^l \quad \text{and} \quad s_k^u = s_{i+1}^u,$$

define

$$s_k^p = \max \left[1, \frac{\|s_k^u\|_\infty}{\|s_k^l\|_\infty} \right] s_k^l,$$

apply the RS Algorithm to find a GCP x_k^C and STOP.

For the computation of s_i in Step 1, we have implemented a self-contained routine that uses the same data structure as that representing problem (1.1) and is a particular implementation of the simplex algorithm specialized to network problems, along the lines described in [2], [16] and [17]. This routine includes at each iteration the computation of the vectors π_r and μ_r from (2.19) as well as the update of the upper bound on the value of $\mu_3 \alpha_k(t_i)$ given in (2.18), and stops as soon as an appropriate inexact solution is computed. This implementation provides in particular a *total pricing* routine (see [17]) for seeking a nonbasic candidate to enter the basis, since the vector μ_r has to be totally evaluated at each iteration. In order to compare the performances of this last algorithm with one that completely solves problem (2.12) (as required if μ_3 is set to 1), we have also implemented a routine that finds the exact solution of (2.12), without adding the extra burden of computing the quantities required for an approximate solution (namely μ_r and the upper bound on $\mu_3 \alpha_k(t_i)$), but rather using a *partial pricing* routine to select a nonbasic arc to be moved. More precisely, we select sets of thirty variables taken at regular intervals among the nonbasic variables and test each variable in the successive sets until a candidate to enter the basis is found.

We have left unspecified the parameter $\lambda \in (0, 1)$ in the GCP Algorithm (see Case 1 of Step 3) in order to test the effect of varying its value. Indeed, in order to avoid an excessive number of computations of a candidate step s_i in Step 1 — the most costly calculation of the algorithm — it could be worth to accelerate the branching to the second case of Step 3 by choosing a smaller value for λ than the classical 0.5.

The above algorithm for the calculation of a GCP has the advantage of avoiding the repeated computation of the projection on the feasible domain, which is a *quadratic* program. Instead we repeatedly compute an approximate solution of *linear* programs. This can be related to the convex combination algorithm originally suggested by Frank and Wolfe (see [20]) for solving quadratic programming problems with linear constraints. The Frank and Wolfe algorithm is based on finding a descent direction by minimizing a linear approximation to the function subject to the linear constraints. A linesearch on the quadratic objective function along the descent direction found is then performed to determine the next iterate.

2.3. The candidate step s_k . In this section, we develop an algorithm for solving problem (2.4), or more precisely, for finding an approximate solution to the reduced equation

$$(2.23) \quad Z^T H_k Z [s]_{\mathcal{S}} = -Z^T g_k.$$

The strategy considered uses a *truncated conjugate gradient* technique, starting from the GCP, which handles the bound constraints

$$(2.24) \quad l_k \leq x_k + s \leq u_k$$

during the conjugate gradient iteration.

The conjugate gradient method is well suited to solve (2.23) without forming the reduced Hessian $Z^T H_k Z$ (which may be considerably denser than both Z and H_k), since it only requires matrix-vector products of the form $Z^T H_k Z v$. These products can be computed relatively cheaply by forming, in turn, $v_1 = Z v$, $v_2 = H_k v_1$ and $v_3 = Z^T v_2$. This is all the cheaper here as a sparse Hessian H_k and a sparse representation of Z can be stored, due to the partially separable structure of the objective f and the structure of the matrix Z (see (2.8) and (2.10)).

The *TCG Algorithm* terminates the conjugate gradient iteration in the solution of (2.23) at the point $x = x_k + s$ whenever:

- The *reduced residual norm* at x (i.e. the norm of the reduced gradient of the model at the point x) is small enough, that is

$$\|Z^T H_k Z [s]_{\mathcal{S}} + Z^T g_k\|_2 \leq \eta_k,$$

where

$$(2.25) \quad \eta_k = \max[\sqrt{\epsilon_M}, \min[0.01, \|Z^T g_k\|_2]] \|Z^T g_k\|_2$$

and ϵ_M is the relative machine precision. This stopping rule allows for better and better approximations to the solution of the Newton equation (2.23) when close to a local minimizer of problem (1.1) and is the essence of a *truncated* Newton scheme.

- $\mathcal{S} = \emptyset$, i.e. there is no way to better refine the current solution x .
- A direction of negative curvature has been encountered.
- An excessive number of iterations has been taken.

The main characteristics of the TCG Algorithm are the following. At each recurrence of a conjugate gradient iteration, the TCG Algorithm will verify if feasibility with respect to the bound constraints (2.24) is still respected. In the case where a bound is reached, the conjugate gradient iteration is temporarily stopped and the current maximal spanning tree is possibly updated, depending on the type of bound encountered. Thereafter, the active set is updated according to the decomposition (2.5), where the index set \mathcal{S} corresponds to the arcs whose current flow is strictly between the bounds l_k and u_k . The conjugate gradient iteration is then possibly restarted.

Now we specify the TCG Algorithm in more detail. In the description given below, we denote by r the *residual* vector $-(g_k + H_k s)$. For a given vector v and a given partition $\mathcal{B} \cup \mathcal{S} \cup \mathcal{N}$ of the set $\{1, \dots, n\}$, we also define the corresponding *reduced* vector v^r as the vector of \mathbf{R}^n defined componentwise by

$$(2.26) \quad [v^r]_i \stackrel{\text{def}}{=} \begin{cases} 0 & \text{if } i \in \mathcal{B} \cup \mathcal{N}, \\ [Z^T v]_j & \text{if } i \text{ is the } j\text{th element of } \mathcal{S} \text{ (that is the } j\text{th} \\ & \text{superbasic arc)}. \end{cases}$$

TCG Algorithm.

Step 0. Initialization. The GCP, $x_k^C = x_k + s_k^C$, and an initial maximal spanning tree whose indices define the set \mathcal{B} are given. Set $x = x_k^C$ and $r = -(g_k + H_k s_k^C)$.

Step 1. The conjugate gradient iteration. As long as there exist arcs $\notin \mathcal{B}$ which are strictly between the bounds l_k and u_k , we continue the conjugate gradient iteration to further minimize the reduced model of the objective function at the point x_k . Each time a restarting is considered, we redefine the index set \mathcal{S} and equation (2.23) accordingly, and solve this last equation starting from the current point x , until one of the stopping rules mentioned above is satisfied or a bound is encountered.

Step 1.0. Define the active set. Set

$$\mathcal{N} = \mathcal{A}(x, l_k, u_k) \setminus \mathcal{B}$$

and deduce \mathcal{S} from the partition (2.5). If $\mathcal{S} = \emptyset$, go to Step 2. Otherwise, compute the matrices B , S , N and Z from the partition (2.5) and (2.8).

Step 1.1. Restart the conjugate gradient iteration. Now that the subspace where the minimization can take place is fixed (namely the space spanned by the superbasic variables indexed by \mathcal{S}), we can proceed with the conjugate gradient iteration.

Step 1.1.0. Initialization before restarting. Compute the *reduced residual* r^r from (2.26) and the relative accuracy level η_k from equation (2.25). Set $d = 0$, $\beta = 0$ and $\rho_2 = \|r^r\|_2^2$.

Step 1.1.1. Test for the required accuracy. If $\rho_2 \leq \eta_k^2$, go to Step 2.

Step 1.1.2. Conjugate gradient recurrences. Compute

$$[d]_{\mathcal{S}} = [r^r]_{\mathcal{S}} + \beta [d]_{\mathcal{S}},$$

$[d]_{\mathcal{B}}$ from

$$B [d]_{\mathcal{B}} = -S [d]_{\mathcal{S}}$$

and set $d = ([d]_{\mathcal{B}}, [d]_{\mathcal{S}}, 0)$. Compute the vectors $y = H_k d$, y^r from (2.26), and the curvature $\gamma = d^T y$. Find α_1 , the largest value of α for which $l_k \leq x + \alpha d \leq u_k$. If $\gamma \leq 0$, then set

$$x = x + \alpha_1 d$$

and go to Step 1.2. Otherwise, calculate $\alpha_2 = \rho_2 / \gamma$. If $\alpha_2 \geq \alpha_1$, then set

$$x = x + \alpha_1 d$$

$$r = r - \alpha_1 y$$

and go to Step 1.2. Otherwise, set

$$x = x + \alpha_2 d$$

$$r = r - \alpha_2 y$$

$$r^r = r^r - \alpha_2 y^r$$

$$\begin{aligned}\rho_1 &= \rho_2 \\ \rho_2 &= \|r^r\|_2^2 \\ \beta &= \frac{\rho_2}{\rho_1}\end{aligned}$$

and go to Step 1.1.1.

Step 1.2. Update the maximal spanning tree. Update the index set \mathcal{B} in order to keep a maximal spanning tree (see further on). If $\gamma \leq 0$, go to Step 2. Otherwise, go to Step 1.

Step 2. Termination of the conjugate gradient iteration. Set

$$s_k = x - x_k.$$

In order to maintain a maximal spanning tree when a pivoting step is required, we need to take into account the bound constraints of both problem (1.1) and problem (2.4) (the latter varying from one iteration to the other, depending on the trust region size), since the spanning tree has to remain maximal with respect to the bounds l and u and l_k and u_k . As illustrated by the following example, it is not sufficient to only consider the maximality of the spanning tree with respect to the bounds l_k and u_k . Suppose indeed, when moving to a point x , that the basic arc of index i hits a bound such that not only $i \in \mathcal{A}(x, l_k, u_k)$, but also $i \in \mathcal{A}(x, l, u)$, and that no arc $j \notin \mathcal{B}$ satisfying $[l_k]_j < [x]_j < [u_k]_j$ may be found to pivot with. In that case, if the current maximal spanning tree remains unmodified and if there exists an arc of index j , say, such that $j \in \mathcal{A}(x, l_k, u_k)$, $i \in \beta_j$ (i.e. arc i belongs to the flow augmenting path of arc j), but $j \notin \mathcal{A}(x, l, u)$, this spanning tree will not be maximal any more with respect to the bounds l and u as soon as the trust region constraint vanishes from (2.4) or is modified. Therefore, based on the observation that $i \in \mathcal{A}(x, l, u) \implies i \in \mathcal{A}(x, l_k, u_k)$ and $j \notin \mathcal{A}(x, l_k, u_k) \implies j \notin \mathcal{A}(x, l, u)$, we consider the following algorithm for maintaining a maximal spanning tree: If, for some $i \in \mathcal{B}$,

$$i \in \mathcal{A}(x, l, u)$$

or

$$i \notin \mathcal{A}(x, l, u) \text{ and } i \in \mathcal{A}(x, l_k, u_k),$$

then determine (if possible) $j \notin \mathcal{B}$ such that $i \in \beta_j$, $\min \left[|[x]_j - [l_k]_j|, |[x]_j - [u_k]_j| \right]$ is maximum and either

$$j \notin \mathcal{A}(x, l, u)$$

or

$$j \notin \mathcal{A}(x, l_k, u_k),$$

respectively. Then redefine the set \mathcal{B} by

$$\mathcal{B} = \mathcal{B} \setminus \{i\} \cup \{j\}$$

and update the submatrix B accordingly, performing a pivoting step as described in [2].

Note that the choice of j in the above description is intended to allow larger steps in the next search, which may result in a more useful decrease of the cost function (see [21]).

2.4. Optimality test. We consider that optimality for problem (1.1) is reached whenever the objective function cannot be further reduced at the current iterate x_k . This may be checked in the following manner.

- Select the arcs that allow for a possible improvement. This amounts to finding the arcs $\notin \mathcal{B}$ which are either strictly between the bounds l and u or at one of these bounds, but whose release may induce a decrease in the objective function. (These last arcs are found through an examination of the corresponding Lagrange multipliers.)
- Remove the so-called *blocked* arcs ([11]), that is the arcs at a bound l or u whose release causes the immediate violation of another bound l or u for one of the arcs of their flow augmenting path. This may be easily verified using the following test:

If arc j is such that, either

$$[x_k]_j = [u]_j \quad \text{and} \quad \exists i \in \beta_j \quad \text{such that}$$

$$([-B^{-1}N]_{ij} = 1 \quad \text{and} \quad [x_k]_i = [l]_i) \quad \text{or} \quad ([-B^{-1}N]_{ij} = -1 \quad \text{and} \quad [x_k]_i = [u]_i),$$

or

$$[x_k]_j = [l]_j \quad \text{and} \quad \exists i \in \beta_j \quad \text{such that}$$

$$([-B^{-1}N]_{ij} = 1 \quad \text{and} \quad [x_k]_i = [u]_i) \quad \text{or} \quad ([-B^{-1}N]_{ij} = -1 \quad \text{and} \quad [x_k]_i = [l]_i),$$

then it is blocked.

(Note that this situation cannot occur for the arcs that are strictly between the bounds l and u , because of the properties of the maximal spanning tree.)

- Denoting by \mathcal{S} the set of indices obtained from the above selection, deduce the set \mathcal{N} from the partition (2.5) and define an active set accordingly.
- Check if the current iterate x_k is optimal on this active set, that is, if the corresponding reduced gradient at x_k is null.

This framework may be summarized by the following algorithm.

OT Algorithm.

Step 0. \mathcal{B} is given. Set $\mathcal{S} = \emptyset$ and $\mathcal{N} = \{1, \dots, n\} \setminus \mathcal{B}$.

Step 1. For each $j \in \{1, \dots, n\} \setminus \mathcal{B}$, redefine \mathcal{S} and \mathcal{N} in the following way. If

$$j \notin \mathcal{A}(x_k, l, u),$$

then redefine \mathcal{S} and \mathcal{N} by

$$\mathcal{S} = \mathcal{S} \cup \{j\} \quad \text{and} \quad \mathcal{N} = \mathcal{N} \setminus \{j\}.$$

Otherwise, compute the Lagrange multiplier estimate associated with the j th variable, namely

$$[\sigma]_j = [g_k]_j + \sum_{i \in \beta_j} [-B^{-1}N]_{ij} [g_k]_i.$$

If $[x_k]_j$ is not potentially blocked (see above), and if either

$$[\sigma]_j < 0 \quad \text{and} \quad [x_k]_j = [l]_j$$

or

$$[\sigma]_j > 0 \text{ and } [x_k]_j = [u]_j,$$

then redefine \mathcal{S} and \mathcal{N} by

$$\mathcal{S} = \mathcal{S} \cup \{j\} \text{ and } \mathcal{N} = \mathcal{N} \setminus \{j\}.$$

Step 2. Compute the matrices B , S , N and Z from the partition (2.5) and (2.8). If $\mathcal{S} = \emptyset$ or

$$\|Z^T g_k\|_\infty \leq \eta_3,$$

STOP (x_k is a local optimum within the required accuracy).

The constant η_3 whose choice controls the final accuracy requirement will be specified later.

2.5. The specific algorithm. We are now in position to specify our trust region algorithm for nonlinear network optimization in its entirety.

TRNNO Algorithm.

Step 0. The bounds l and u , the vector b and the network associated with the matrix A are given. Compute a feasible starting point x_0 (if not given) and an initial trust region radius Δ_0 . Compute $f(x_0)$, g_0 and H_0 . Find an initial maximal spanning tree of the network, defining a set of basic indices \mathcal{B} . Set $k = 0$.

Step 1. Given η_3 , test the optimality of the current iterate x_k using the OT Algorithm of §2.4 and STOP if x_k is optimal.

Step 2. Calculate the bounds l_k and u_k from equation (2.3). Given μ_3 , find a Generalized Cauchy Point x_k^C using the GCP Algorithm detailed in §2.2. (Also include an updating phase for the maximal spanning tree.)

Step 3. Compute the active set $\mathcal{A}(x_k^C, l_k, u_k)$ and apply the TCG Algorithm proposed in §2.3, using a truncated conjugate gradient scheme, to find an approximation $x_k + s_k$ to the minimizer of the trust region problem (2.4), with the additional restriction that the variables whose indices are in $\mathcal{A}(x_k^C, l_k, u_k)$ remain fixed at the corresponding values of x_k^C . (Also include an updating phase for the maximal spanning tree.)

Step 4. Compute $f(x_k + s_k)$ and

$$\rho_k = \frac{f(x_k) - f(x_k + s_k)}{m_k(x_k) - m_k(x_k + s_k)}.$$

Step 5. If $\rho_k > \eta_1$, then set

$$x_{k+1} = x_k + s_k$$

and update g_{k+1} and H_{k+1} accordingly. Otherwise, set

$$x_{k+1} = x_k$$

and update the maximal spanning tree (with respect to the bounds l and u only). Set Δ_{k+1} according to equation (2.2), increment k by one and go to Step 1.

3. Numerical experiments. In this section, we analyse and compare the various versions of our algorithm and we also briefly interpret our results when varying the storage scheme, the conditioning, the dimension and the nonlinearity of the problem, the final accuracy level (η_3) and the type of bounds imposed on the variables, as in [21] and [22]. We then consider our algorithm in comparison with the LSNNNO¹ routine, developed by Toint and Tuytens in [21]–[22], that uses a linesearch approach rather than a trust region approach to solve problem (1.1). Although it might have been instructive to compare the present algorithm with another such as GENOS [1] and an interior point method like [3], the amount of additional work would have been prohibitive and we preferred to use a competitive algorithm for which we had direct access to both the authors and the software.

We have experimented on all the test problems of [21] for which the first and second derivatives were available. Indeed, though the framework presented here is well suited to large dimensional problems and can be used in conjunction with partitioned secant updating techniques on the general class of partially separable problems (see [14] and [15]), the purpose of this paper is to show the viability of the framework proposed and studied in [4], as well as its efficiency on large-scale nonlinear problems. Consequently, the results are presented for problems with easily computable first and second derivatives. For the same reason, we did not consider any preconditioning in our present implementation.

We have mainly tested problems obtained by varying the five parameters of the so-called model test problem $P(\ell, a, c, i, r)$ constructed by Toint and Tuytens [21], where:

ℓ defines the number of arcs $n = 2(2\ell + 1)(2\ell + 2)$ and the number of nodes $n_n = (2\ell + 2)^2$ of the problem;

a defines the nonlinearity of the function (for $a = 0$ the function is a simple quadratic);

c is an estimate of the condition number of the objective's Hessian matrix projected in the subspace of variables that satisfy the network constraints;

i and r determine a specific set of bounds on the flows (for $i = 0$ no bounds are imposed, for $i = 1$ a lower bound equal to r is imposed on the flows whose index is a multiple of three, for $i = -1$ some flows are fixed while others are bounded, principally those on the border of the grid with lower bound equal to r).

A brief description of this model test problem follows, the reader being referred to [21] for more details. The network is constructed as a square planar grid. An example with $\ell = 2$ is shown in Fig. 1. The supply/demand vector is

$$b_1 = +10, \quad b_j = 0 \quad (j = 2, \dots, n_n - 1), \quad b_{n_n} = -10.$$

Furthermore, sets of ℓ horizontal cycles and ℓ vertical cycles are distinguished in the grid (see the dashed lines in the example of Fig. 1). We define, for $i = 1, \dots, n$,

$$j(i) \stackrel{\text{def}}{=} \begin{cases} s & \text{if the } i\text{th arc belongs to cycle } s \text{ (horizontal or vertical),} \\ 0 & \text{if the } i\text{th arc does not belong to any cycle.} \end{cases}$$

The objective function is then given by

$$(3.1) \quad f(x) = \frac{1}{100} \sum_{i=1}^n \alpha_i [x]_i^2 + \frac{a}{100} \left(\sum_{i=1}^{n-1} \sqrt{1 + [x]_i^2 + ([x]_i - [x]_{i+1})^2} + \frac{1}{1200} [10 + \sum_{i=1}^n (-1)^i [x]_i]^4 \right),$$

¹ LSNNNO is available from NETLIB.

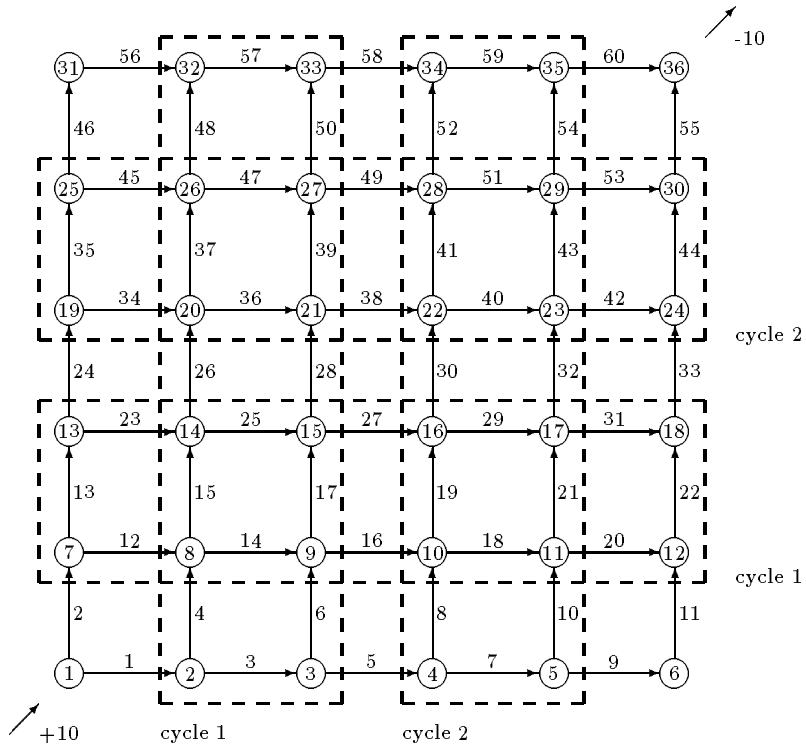


FIG. 1. The network of the model test problem for $\ell = 2$

TABLE 1
Dembo's test problems

| Name | n | n_n | Description |
|--------|------|-------|--|
| W30 | 46 | 30 | Small Dallas water distribution model |
| W150 | 196 | 150 | Medium Dallas water distribution model |
| W666 | 906 | 666 | Large Dallas water distribution model |
| MB64 | 117 | 64 | Small Thai matrix balancing problem |
| MB1116 | 2230 | 1116 | Large Thai matrix balancing problem |

where

$$\alpha_i \stackrel{\text{def}}{=} \begin{cases} 10^{\frac{j(i)-1}{i-1} \log_{10} c} & \text{if } j(i) \geq 1, \\ 1 & \text{if } j(i) = 0. \end{cases}$$

We have also tested the so-called Dembo's test problems given by Dembo in [11]. These problems are summarized in Table 1 (where n denotes the number of arcs and n_n denotes the number of nodes). All of them are *totally* separable, convex and rather ill-conditioned (the condition number of the reduced Hessian at the solution varying between 10^4 and 10^8), and the number of bounds active at the solution is small, compared to n .

All the computations have been performed in double precision on a DEC VAX 3500, under VMS, using the standard Fortran Compiler ($\epsilon_M \simeq 1.39 \times 10^{-17}$).

The tests reported below all use the following values for the algorithm's constants

(suggested in [4]):

$$\eta_1 = 0.25 \text{ and } \eta_2 = 0.75, \quad \mu_1 = 0.1 \text{ and } \mu_2 = 0.9, \quad \nu_1 = 10^{-5} \text{ and } \nu_2 = 0.01.$$

In order to allow the initial parameter t_0 in the GCP Algorithm to be more refined than Δ_k itself (since this last value represents a trust region radius for the quadratic model much more than for the linear model used in Step 1), we have selected the following value,

$$(3.2) \quad t_0 = \min \left[\left| \frac{g_k^T g_k}{g_k^T H_k g_k} \right| \|g_k\|_\infty, \Delta_k \right],$$

where the first quantity in brackets is the distance from x_k to the minimum of the quadratic model in the steepest descent direction, computed in the infinity norm. The value of μ_3 in the GCP Algorithm (that can be interpreted as the level of solution of the linear network problem (2.12)) is specified for each table of results given below. We have chosen the value 0.1 (rather than the classical value 0.5) for the scalar λ in the GCP Algorithm. This is intended to speed up the branching to the second case of Step 3 in this algorithm, therefore possibly reducing the number of times a candidate step s_i is computed in Step 1, since this last calculation is expected to be expensive compared with the rest of the algorithm. The final accuracy level η_3 in the OT Algorithm is specified for each model problem and is set to 10^{-2} for the Dembo's test problems, as recommended in [11]. In all cases, the (possibly infeasible) starting point is the origin. A feasible starting point x_0 as required in the statement of the TRNNO Algorithm is then computed via an "all artificial start Phase 1" (see [21]). This allows comparison with the LSNNO routine that starts with the same point. (Note that since the cpu-time for the computation of this point, when required, is always negligible compared with the overall cpu-time, it will be ignored in the cpu-times given in the tables.) Finally, the initial trust region radius is fixed to the following value in our tests:

$$(3.3) \quad \Delta_0 = \min[\|g_0\|_2, 100].$$

3.1. Comparison between the different versions. In this section we comment on the five Dembo's test problems and on twenty others selected from particular choices in [21]–[22] of the model test problem's parameters. Table 2 reports the characteristics of these twenty test problems which are divided into six subsets, according to the different features tested in [21]–[22] and mentioned above. Note that the symbols I , E and O in the last column of this table are used to denote storage using internal dimensions (I), elemental dimensions (E) or using one element (O) for the Hessian matrix (see [21]–[22] for more details). When required for comparisons in the next section, we report the relevant numerical results of all the twenty tests, even if some of these are identical (namely MP6, MP11, MP16 and MP19).

We introduce the notation used in the tables presenting the results:

- it: the number of major iterations (in the TRNNO Algorithm of §2.5);
- gcp: the total number of iterations in the GCP calculations;
- avn: the average number of GCP calculations per major iteration;
- cg: the total number of conjugate gradient recurrences;
- nf: the number of function evaluations (i.e. the number of element function evaluations divided by the number of elements);
- ng: the number of gradient evaluations (i.e. the number of element gradient evaluations divided by the number of elements);

TABLE 2
The model test problems

| | Name | ℓ | a | c | i | r | η_3 | storage |
|----------------|------|--------|-----|--------|-----|----------------|-----------|---------|
| Storage scheme | MP1 | 8 | 1 | 10^3 | -1 | $\frac{1}{10}$ | 10^{-5} | I |
| | MP2 | 8 | 1 | 10^3 | -1 | $\frac{1}{10}$ | 10^{-5} | E |
| | MP3 | 8 | 1 | 10^3 | -1 | $\frac{1}{10}$ | 10^{-5} | O |
| Conditioning | MP4 | 8 | 1 | 1 | 1 | $\frac{1}{10}$ | 10^{-5} | I |
| | MP5 | 8 | 1 | 10 | 1 | $\frac{1}{10}$ | 10^{-5} | I |
| | MP6 | 8 | 1 | 10^2 | 1 | $\frac{1}{10}$ | 10^{-5} | I |
| | MP7 | 8 | 1 | 10^3 | 1 | $\frac{1}{10}$ | 10^{-5} | I |
| | MP8 | 8 | 1 | 10^4 | 1 | $\frac{1}{10}$ | 10^{-5} | I |
| | MP9 | 8 | 1 | 10^5 | 1 | $\frac{1}{10}$ | 10^{-5} | I |
| Dimension | MP10 | 4 | 1 | 10^2 | 1 | $\frac{1}{10}$ | 10^{-5} | I |
| | MP11 | 8 | 1 | 10^2 | 1 | $\frac{1}{10}$ | 10^{-5} | I |
| | MP12 | 12 | 1 | 10^2 | 1 | $\frac{1}{10}$ | 10^{-5} | I |
| Nonlinearity | MP13 | 8 | 0 | 10^2 | 1 | $\frac{1}{10}$ | 10^{-5} | I |
| | MP14 | 12 | 0 | 10^2 | -1 | $\frac{1}{10}$ | 10^{-5} | I |
| Final accuracy | MP15 | 8 | 1 | 10^2 | 1 | $\frac{1}{10}$ | 10^{-3} | I |
| | MP16 | 8 | 1 | 10^2 | 1 | $\frac{1}{10}$ | 10^{-5} | I |
| | MP17 | 8 | 1 | 10^2 | 1 | $\frac{1}{10}$ | 10^{-7} | I |
| Type of bounds | MP18 | 8 | 1 | 10^2 | 0 | 0 | 10^{-5} | I |
| | MP19 | 8 | 1 | 10^2 | 1 | $\frac{1}{10}$ | 10^{-5} | I |
| | MP20 | 8 | 1 | 10^2 | 1 | $\frac{1}{5}$ | 10^{-5} | I |

nH: the number of Hessian evaluations (i.e. the number of element Hessian evaluations divided by the number of elements);

np: the number of maximal spanning tree updates where a pivoting step occurs;

gcpcpu: the cpu-time in seconds for the GCP calculations;

cgcpu: the cpu-time in seconds for the conjugate gradient recurrences;

totcpu: the total cpu-time in seconds (Phase 1 excluded).

Note that fractional numbers of function, gradient or Hessian evaluations are expected, since the partial separability of the objective allows skipping the re-evaluation of the elements whose variables have not been modified since the last evaluation. On the other hand, for the sake of clarity, we round off the cpu-times to the nearest integer number.

We first turn our attention to the computation of a candidate step s_i at Step 1 of the GCP Algorithm. As already mentioned in §2.2, we have implemented a *total pricing* routine that *approximately* solves problem (2.12). We have tested this routine for different values of μ_3 . The results are presented in Table 3 for a representative sample of the twenty-five problems.

We first observe that the number of major iterations usually increases when the value of μ_3 decreases (especially for $\mu_3 = 0.6$). The reason is that for smaller and smaller values of μ_3 , the GCP is allowed to be chosen further and further from the projected gradient path. This exhibits the importance of the part played by the GCP in our class of trust region methods and the need of computing a sufficiently good approximation of this point on the projected gradient path. The total number of GCP iterations increases accordingly. However, we observe that the average number of GCP calculations per major iteration decreases with the value of μ_3 , while the cpu-times for the GCP calculations considerably decrease, particularly for larger problems (such as MP12, MP14, W666 and MB1116). This is due to the fact that the solution

TABLE 3
Total pricing, $\mu_3 = 1, 0.9$ and 0.6

| Problem | μ_3 | it | gcp | avn | cg | gpcpu | cgcpu | totcpu |
|---------|---------|----|-----|-----|-------|-------|-------|--------|
| MP4 | 1 | 11 | 31 | 2.8 | 587 | 118 | 110 | 241 |
| | 0.9 | 11 | 31 | 2.8 | 564 | 103 | 106 | 223 |
| | 0.6 | 11 | 31 | 2.8 | 530 | 78 | 99 | 190 |
| MP8 | 1 | 7 | 30 | 4.3 | 2433 | 60 | 441 | 510 |
| | 0.9 | 9 | 43 | 4.8 | 3315 | 63 | 607 | 681 |
| | 0.6 | 11 | 47 | 4.3 | 3475 | 31 | 619 | 663 |
| MP12 | 1 | 7 | 28 | 4.0 | 1078 | 333 | 479 | 833 |
| | 0.9 | 8 | 34 | 4.2 | 1254 | 280 | 554 | 857 |
| | 0.6 | 9 | 31 | 3.4 | 1125 | 88 | 489 | 602 |
| MP14 | 1 | 5 | 16 | 3.2 | 291 | 30 | 29 | 68 |
| | 0.9 | 6 | 24 | 4.0 | 357 | 20 | 35 | 66 |
| | 0.6 | 13 | 39 | 3.0 | 603 | 12 | 58 | 88 |
| MP16 | 1 | 8 | 30 | 3.7 | 815 | 83 | 152 | 244 |
| | 0.9 | 8 | 29 | 3.6 | 871 | 70 | 164 | 243 |
| | 0.6 | 8 | 27 | 3.4 | 726 | 49 | 134 | 193 |
| MP18 | 1 | 12 | 45 | 3.7 | 823 | 113 | 166 | 295 |
| | 0.9 | 12 | 45 | 3.7 | 810 | 109 | 164 | 288 |
| | 0.6 | 12 | 45 | 3.7 | 827 | 78 | 166 | 260 |
| W150 | 1 | 15 | 61 | 4.1 | 362 | 6 | 5 | 16 |
| | 0.9 | 15 | 61 | 4.1 | 405 | 5 | 6 | 14 |
| | 0.6 | 18 | 73 | 4.1 | 442 | 3 | 6 | 14 |
| W666 | 1 | 19 | 97 | 5.1 | 1314 | 247 | 110 | 385 |
| | 0.9 | 21 | 108 | 5.1 | 1890 | 146 | 159 | 334 |
| | 0.6 | 26 | 130 | 5.0 | 2076 | 64 | 162 | 260 |
| MB1116 | 1 | 39 | 60 | 1.6 | 15039 | 2834 | 4632 | 7541 |
| | 0.9 | 40 | 57 | 1.4 | 13806 | 1886 | 3643 | 5599 |
| | 0.6 | 40 | 57 | 1.4 | 14587 | 1481 | 4739 | 6302 |

of the linear network problem (2.12) may be stopped prematurely when finding an approximate solution. Nevertheless, comparing the total cpu-times, we conclude that it is worthwhile solving (2.12) approximately whenever the GCP found does not depart too much from the projected gradient path and the total number of iterations is largely unaffected (see MP4, MP16 and MP18). This means that the value of μ_3 must be reduced with care.

We have also tested the *partial pricing* routine that *completely* solves problem (2.12) (hence setting $\mu_3 = 1$). These results are reported in Table 4. The total cpu-times are better than those given in Table 3. This is due to much better cpu-times for the GCP calculations. Indeed, problems MP4 and MP18 for instance present similar numbers of GCP calculations and yet, the exact solution's calculation using partial pricing is less expensive than the approximate solution's calculation, even when $\mu_3 = 0.6$. This can be explained by the additional amount of work required for maintaining the upper bound on the value of $\mu_3 \alpha_k(t_i)$ in (2.18) when approximately solving (2.12). This additional work is not sufficiently balanced by the use of the upper bound and leads to the conclusion that it is not worth solving approximately the linear problem (2.12) in the GCP calculation, at least in the presence of *network* constraints, since a fast solver can then be implemented to solve problem (2.12) exactly. We therefore abandon, from now on, the approximate solution of (2.12) in favour of the

TABLE 4
Partial pricing, $\mu_3 = 1$

| Problem | it | nf | ng | nH | np | gcp | cg | gcpcpu | cgcpu | totcpu |
|---------|----|------|------|------|-----|-----|-------|--------|-------|--------|
| MP1 | 6 | 5.9 | 5.9 | 5.0 | 0 | 27 | 393 | 8 | 63 | 79 |
| MP2 | 6 | 5.9 | 5.9 | 5.0 | 0 | 27 | 402 | 53 | 628 | 709 |
| MP3 | 6 | 7.0 | 7.0 | 6.0 | 0 | 27 | 400 | 50 | 571 | 649 |
| MP4 | 11 | 11.3 | 11.3 | 10.4 | 6 | 31 | 583 | 22 | 111 | 147 |
| MP5 | 9 | 9.5 | 9.5 | 8.5 | 4 | 29 | 683 | 18 | 133 | 163 |
| MP6 | 8 | 8.5 | 8.5 | 7.5 | 5 | 30 | 816 | 17 | 154 | 182 |
| MP7 | 8 | 8.5 | 8.5 | 7.5 | 5 | 36 | 1610 | 19 | 306 | 334 |
| MP8 | 7 | 7.5 | 7.5 | 6.6 | 5 | 31 | 2450 | 15 | 453 | 477 |
| MP9 | 10 | 10.3 | 10.3 | 9.3 | 3 | 50 | 6649 | 24 | 1260 | 1297 |
| MP10 | 5 | 5.6 | 5.6 | 4.7 | 3 | 17 | 190 | 2 | 10 | 14 |
| MP11 | 8 | 8.5 | 8.5 | 7.5 | 5 | 30 | 816 | 17 | 154 | 182 |
| MP12 | 7 | 7.5 | 7.5 | 6.6 | 54 | 28 | 1116 | 39 | 492 | 551 |
| MP13 | 5 | 5.4 | 5.4 | 4.5 | 7 | 19 | 521 | 7 | 37 | 49 |
| MP14 | 5 | 3.7 | 3.7 | 3.1 | 3 | 16 | 295 | 6 | 29 | 44 |
| MP15 | 7 | 7.5 | 7.5 | 6.5 | 5 | 23 | 713 | 14 | 134 | 157 |
| MP16 | 8 | 8.5 | 8.5 | 7.5 | 5 | 30 | 816 | 17 | 155 | 182 |
| MP17 | 9 | 9.5 | 9.5 | 8.5 | 5 | 39 | 1024 | 21 | 196 | 227 |
| MP18 | 12 | 13.0 | 13.0 | 12.0 | 0 | 45 | 809 | 24 | 166 | 206 |
| MP19 | 8 | 8.5 | 8.5 | 7.5 | 5 | 30 | 816 | 17 | 155 | 182 |
| MP20 | 7 | 7.1 | 7.1 | 6.2 | 7 | 30 | 631 | 12 | 112 | 133 |
| W30 | 15 | 13.9 | 13.9 | 13.0 | 1 | 72 | 113 | 1 | 1 | 2 |
| W150 | 15 | 12.4 | 12.4 | 11.6 | 4 | 61 | 351 | 4 | 5 | 13 |
| W666 | 16 | 15.1 | 15.1 | 14.2 | 6 | 79 | 1087 | 37 | 91 | 151 |
| MB64 | 55 | 50.6 | 50.6 | 49.6 | 42 | 56 | 2551 | 8 | 30 | 43 |
| MB1116 | 36 | 23.4 | 23.4 | 22.6 | 142 | 55 | 12823 | 255 | 4064 | 4391 |

exact one using partial pricing.

We now further analyse the results reported in Table 4 for the twenty-five test problems. The number of iterations used in the GCP calculations are generally quite reasonable when compared with the number of major iterations or with the total number of conjugate gradient recurrences. The same conclusion applies when comparing the respective cpu-times. This is partly due to the choice of a small value for λ in the GCP Algorithm. Indeed, we have tested the same code with $\lambda = 0.1$ replaced by $\lambda = 0.5$, and we have clearly detected a substantial increase in the number of iterations and the cpu-times for the GCP calculations. This thus justifies a choice for λ that allows a rapid branching to the RS Algorithm (Case 2 of Step 3 in the GCP Algorithm), therefore avoiding an unnecessarily high number of solutions of the linear network problem (2.12). Moreover, we also observe that the amount of work in the GCP calculations grows more slowly with the size of the problem than in the conjugate gradient scheme (compare MP10, MP11 and MP12 or the Dembo's problems, for instance). This is true for the number of iterations as well as for the cpu-times.

We have also tested the impact of the choice of the initial trust region radius Δ_0 on the performances of the method. Indeed, the initial value given in (3.3) is rather heuristic, and we actually observed that eighteen on the twenty-five test problems selected $\Delta_0 = 100$. Table 5 reports the results obtained when solving problem MB1116 for different initial trust region radii, with the GCP Algorithm with $\mu_3 = 1$ (economical version). These results, compared with those of Table 4, show a possible

TABLE 5
The effect of varying the initial trust region radius for MB1116

| Δ_0 | it | gcp | cg | gpcpu | cgcpu | totcpu |
|------------|----|-----|-------|-------|-------|--------|
| 10^5 | 35 | 55 | 10166 | 243 | 3033 | 3343 |
| 10^9 | 34 | 56 | 10805 | 241 | 3373 | 3678 |
| 10^{14} | 34 | 57 | 10645 | 240 | 3238 | 3542 |
| 10^{18} | 34 | 57 | 10645 | 239 | 3244 | 3547 |

saving of up to 25% in the total cpu-times, depending only on the value of Δ_0 . This saving occurs essentially in the conjugate gradient iteration counts. This emphasizes the importance of a good choice for this last value.

3.2. Variation of the test problems' features. We briefly interpret here our results on the twenty model test problems of §3.1 when varying the six items mentioned at the beginning of §3. The reader is invited to consult Table 4 in order to confirm the comments given below.

We first observe essentially identical behaviour for the method of this manuscript and that of [22] when using the three different storage schemes for the Hessian matrix (see MP1 to MP3). Our cpu-times are clearly in favour of the internal storage technique, although, for example, the additional subroutine calls necessary in this context can be quite significant. We also observe a small increase in function, gradient and Hessian counts when going from the elemental dimension storage to that of one element, the number of conjugate gradient steps and the iteration counts being approximately unchanged. This effect is due to the loss of the partially separable character of the objective in the latter case, which prevents partial evaluations of the function or of its derivatives. The gains in cpu-time for the storage using one element as opposed to the elemental dimension storage is caused by the fact that the products involving the Hessian matrices are cheaper to compute (see [21]).

We also see, as in [21]–[22], that the method is sensitive to variations of conditioning (see MP4 to MP9). This is due to the use of the conjugate gradient method which is a conditioning sensitive method, and leads to an increase in the numbers of conjugate gradient recurrences (while the GCP calculations remain comparable).

The problem becomes slightly more difficult when its size increases, mostly because of the added complexity of the bound constraints (see for example MP10 to MP12). Nevertheless, the difficulty seems to increase faster in [21] than for our code. This will be confirmed in the next section.

Moreover, when the objective function is quadratic (i.e. when $a = 0$ in Table 2 or in (3.1)), we can say, unlike [21], that the problem is easier in terms of major iterations, function, gradient and Hessian evaluations, as well as in terms of conjugate gradient steps and cpu-times (see MP13 to compare with MP6, and MP14).

As observed in [21]–[22], a tighter requested accuracy on the solution does not cause a large increase in the number of major iterations (see MP15 to MP17). This is explained by the rapid rate of convergence achieved by both methods. The number of conjugate gradient recurrences may however be significantly increased by a tighter accuracy requirement, because a large part of this computational effort occurs in the last iterations of the algorithm, where the linear system (2.23) must be solved accurately.

Finally, unlike [21]–[22], we note that the introduction of bounds does not increase the number of major iterations, but even decreases it (see MP18 to MP20). This will

TABLE 6
Number of arcs and nodes for a given ℓ

| ℓ | 11 | 12 | 13 | 14 | 15 | 16 | 19 | 22 |
|--------|------|------|------|------|------|------|------|------|
| n | 1104 | 1300 | 1512 | 1740 | 1984 | 2244 | 3120 | 4140 |
| n_n | 576 | 676 | 784 | 900 | 1024 | 1156 | 1600 | 2116 |

be discussed in the next section. On the other hand, as in [21]–[22], the number of pivoting steps increases with the tightness of the bounds. This is due to the fact that the basic variables are increasingly constrained.

3.3. Comparison with the LSNNO routine. In this section, we compare the TRNNO routine (partial pricing, Δ_0 given by (3.3)) with the LSNNO code of Tuytens, both tested on the same machine.

We first consider the results of Table 4 in comparison with those produced by LSNNO in [21]–[22] when using Newton’s method without preconditioning. We observe, in most cases, a decrease in the number of major iterations for TRNNO (especially for problems MP9 and MP12). This implies fewer function, gradient and Hessian evaluations. On the other hand, the number of conjugate gradient recurrences generally increases, mainly because the TCG Algorithm allows the restarting of the conjugate gradient scheme. So we may conclude that the TRNNO code requires fewer iterations than the LSNNO code, but that one iteration is more expensive for TRNNO, due to the GCP calculations and the restarting steps in the conjugate gradient iterations. For this first set of problems (whose characteristics are summarized in Table 2), we may observe that LSNNO generally outperforms TRNNO in cpu-times, except, in particular, for the large model test problems (MP12 and MP14) and when the bounds on the variables become tighter (MP18 to MP20), that is, when the number of bounds potentially active at the solution increases. In order to investigate this issue further, we have extended our original set of problems and tested both codes on the model test problem for different sizes and types of bounds, with the fixed parameters $a = 1$, $c = 10^2$, $\eta_3 = 10^{-5}$ for the final accuracy, and using a storage with internal dimension (I). This last choice is indeed the most common choice made in the original set of problems (see Table 2). We report the results in Tables 7 to 10 and in Fig. 2 to 8. The various sizes specified by the parameter ℓ are given in Table 6. We have selected three types of bounds:

Case $i = 1$. We impose that $r \leq [x]_j \leq \infty$ for all index j such that $\text{mod}(j,3) = 0$, all other variables being unconstrained. r is successively equal to 0.15, 0.35, 0.55 and 0.75.

Case $i = 2$. We impose that $r \leq [x]_j \leq \infty$ for all index j such that $\text{mod}(j,3) = 1$, all other variables being unconstrained. r is successively equal to 0, 0.5, 1 and 2.5.

Case $i = 3$. We impose that $r \leq [x]_j \leq \infty$ for all index j whose corresponding arc is on horizontal lines or alternate vertical lines (beginning at the first) of the grid, all other variables being unconstrained. r is successively equal to 0, 0.1 and 0.2.

For the two first cases, one third of the variables are constrained while this ratio increases to three quarters for Case $i = 3$.

Firstly we comment on the results given in Table 7 and Fig. 2 and 3 for Case $i = 1$. In Table 7 and the following ones, “%act” denotes the percentage of active bounds at the solution (computed by LSNNO).

The results of Table 7 show that on the whole the number of major iterations decreases when bounds become tighter for TRNNO, as mentioned in the previous

TABLE 7
Comparison with LSNNO for Case $i = 1$

| r | ℓ | it | | %act |
|------|--------|-------|-------|------|
| | | TRNNO | LSNNO | |
| 0.15 | 16 | 13 | 19 | 9.6 |
| | 19 | 9 | 28 | 11.4 |
| | 22 | 17 | 34 | 13.4 |
| 0.35 | 16 | 15 | 18 | 23.3 |
| | 19 | 9 | 32 | 24.6 |
| | 22 | 10 | 66 | 25.1 |
| 0.55 | 16 | 9 | 25 | 26.2 |
| | 19 | 7 | 41 | 26.6 |
| | 22 | 7 | 42 | 27.0 |
| 0.75 | 16 | 5 | 24 | 27.4 |
| | 19 | 8 | 63 | 27.6 |
| | 22 | 7 | 41 | 28.0 |

TABLE 8
Comparison with LSNNO for Case $i = 2$

| r | ℓ | it | | %act |
|-----|--------|-------|-------|------|
| | | TRNNO | LSNNO | |
| 0.0 | 16 | 16 | 11 | 0.6 |
| | 19 | 12 | 19 | 0.7 |
| | 22 | 21 | 29 | 0.7 |
| 0.5 | 16 | 8 | 29 | 26.1 |
| | 19 | 6 | 28 | 26.8 |
| | 22 | 8 | 39 | 27.2 |
| 1.0 | 16 | 10 | 41 | 28.9 |
| | 19 | 7 | 53 | 28.9 |
| | 22 | 7 | 63 | 29.3 |
| 2.5 | 16 | 8 | 50 | 30.9 |
| | 19 | 9 | 42 | 31.1 |
| | 22 | 10 | 103 | 31.3 |

section. On the other hand, these numbers increase for LSNNO. Now comparing the cpu-times given in Fig. 2, we may observe that this behaviour has the effect of improving the performances of TRNNO while those of LSNNO deteriorate. Moreover, we observe that TRNNO outperforms LSNNO for the largest problem first, then for the medium one and finally for the smallest one. Figure 3 once again confirms the above observation. For tighter and tighter bounds, TRNNO produces better and better cpu-times (except for $l = 19$ when going from $r = 0.55$ to $r = 0.75$), while those for LSNNO behave erratically but are consistently worse. Finally, from Fig. 2 and the last column of Table 7, we can see that the cpu-times are overwhelmingly in favour of TRNNO when about a quarter of the bounds are active at optimality.

The second case is reported in Table 8 and Fig. 4 and 5. These results corroborate the conclusions made for the previous case. It further shows (see Fig. 5) how constant the number of iterations for TRNNO remains when the bounds and the size vary, while these numbers grow for LSNNO. Figure 4 displays this characteristic for $l = 22$.

Finally, Table 9 and Fig. 6 show the results for the third case of bounds. The absence of results for LSNNO means that it stopped with a flag error before having

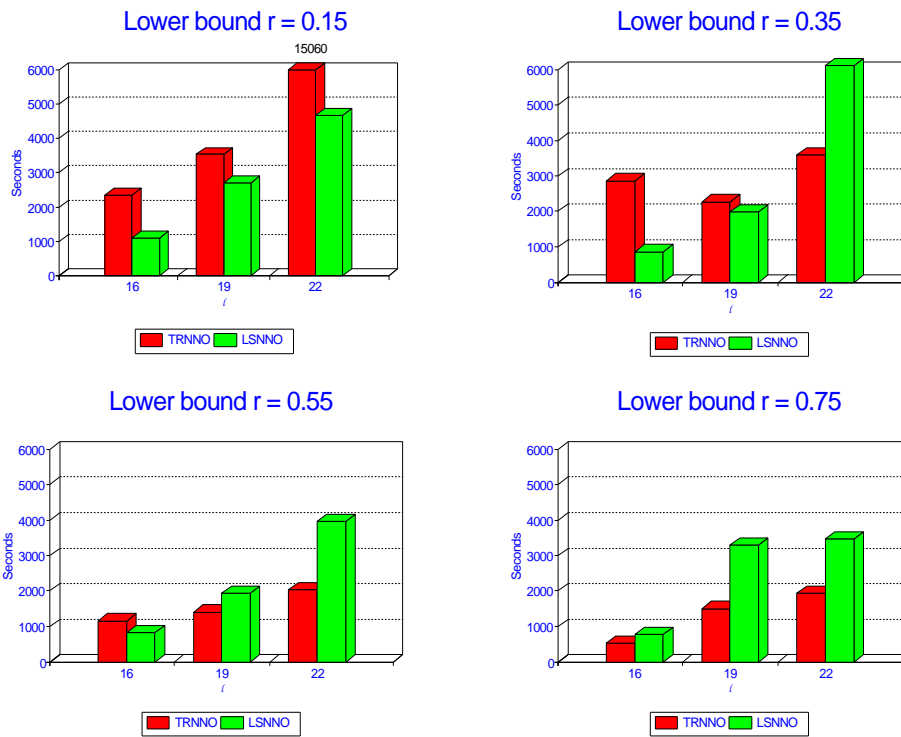


FIG. 2. Comparison with LSNN0 on *cpu-times* for fixed bounds (Case $i = 1$)

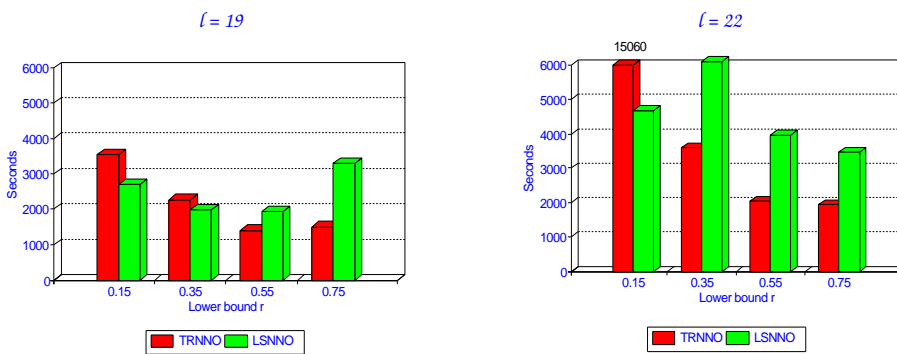


FIG. 3. Comparison with LSNN0 on *cpu-times* for fixed sizes (Case $i = 1$)

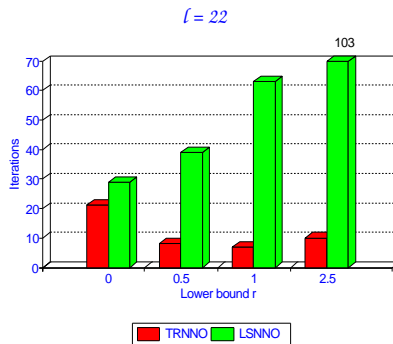


FIG. 4. Comparison with LSNN0 on iterations for fixed size (Case $i = 2$)

solved the problem. The results also confirm the above comments, except that this time TRNNO outperforms LSNN0 immediately, even when about one per cent of the bounds are active at optimality. In particular, Fig. 6 clearly shows the uniform behaviour of TRNNO. Indeed, for the three different bounds, the iterations numbers stay alike while the cpu-times grow slowly with the dimension of the problem. The tightness of the bounds does not seem to affect the performances of the code. On the other hand, it is not possible to attribute the same stability to LSNN0. Moreover, although optimal function values usually agree for both codes in Cases $i = 1$ and 2, we have observed here a significant difference, always in the favor of TRNNO, for three quarters of the test problems. We also observed that the strict complementarity slackness condition did usually not hold at the solution for these problems.

Furthermore for Case $i = 3$, Table 10 and Fig. 7 and 8 report the results for higher dimensions. They confirm the efficiency of TRNNO on large-scale problems. We also tested other cases of bounds which are not reported in this paper. They all corroborate the conclusions made in this section.

4. Conclusions and perspectives. In this paper, we propose a new algorithm of trust region type to solve the nonlinear network problem (1.1). We consider practical implementation issues, including an explicit procedure for computing an approximate Generalized Cauchy Point and a truncated conjugate gradient strategy for calculating a candidate step at each iteration. Numerical tests are reported and discussed, showing the efficiency of the trust region approach, especially for large-scale problems with potentially many active bound constraints at the solution. We believe that part of the success may be attributed to the ability of the GCP calculation to swiftly determine the set of (nondegenerate) active bounds at the solution.

The encouraging results show that the framework presented is worth considering for the solution of problem (1.1), especially in view of the good theoretical properties of the framework given in [4] and the numerical results for large problems. It also suggests some directions for future research and continued development. The method given here could be adapted for solving *general large-scale linearly constrained problems*. We could then envisage to produce effective methods for solving *general large-scale nonlinear programming problems* by combining the nonlinear constraints in a suitable fashion with the objective function (for instance in an augmented Lagrangian function [8], [5], [6]), and solving the resulting sequence of linearly constrained problems using the method described in this paper.

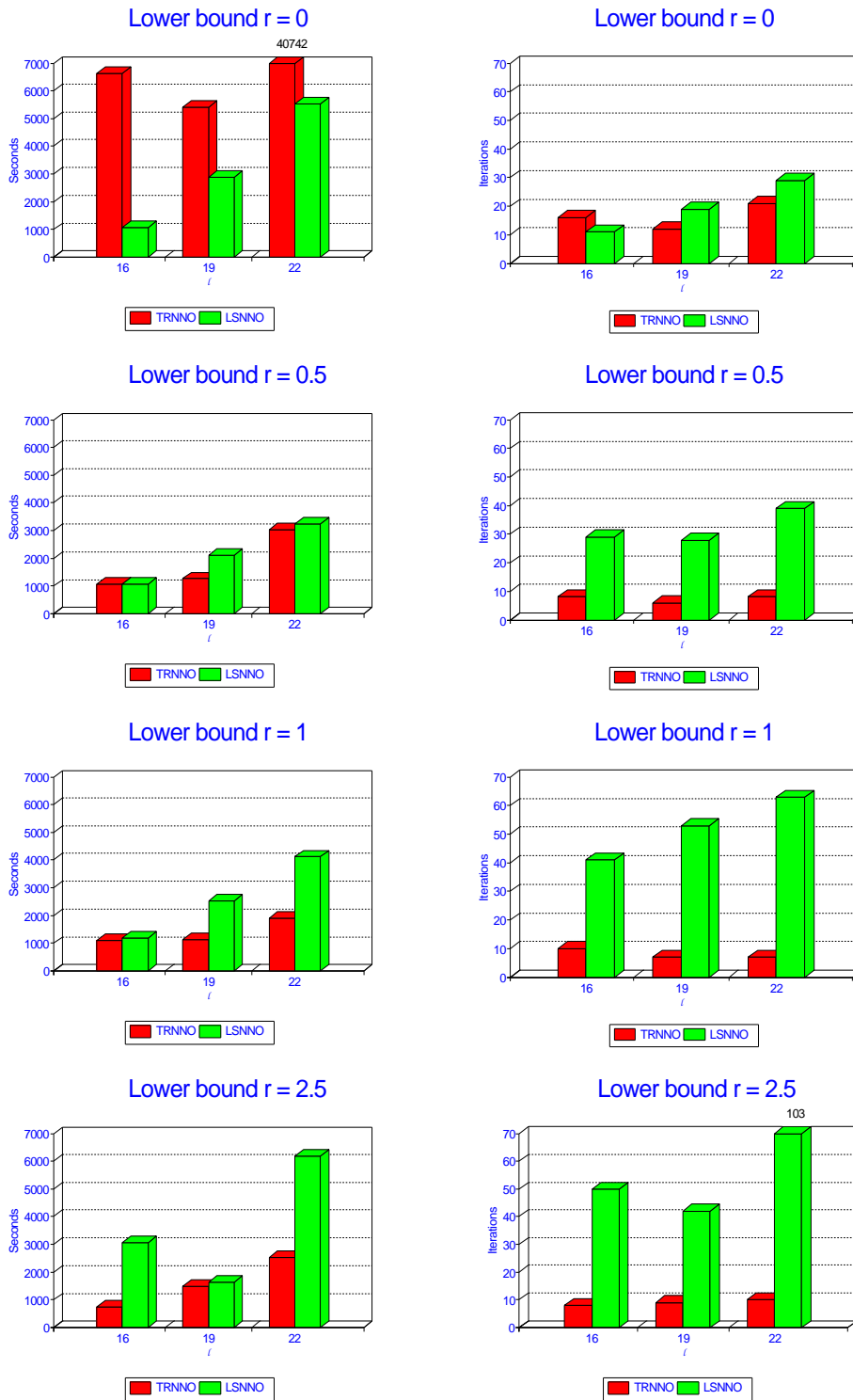


FIG. 5. Comparison with LSNN0 on cpu-times and iterations for fixed bounds (Case $i = 2$)

TABLE 9
Comparison with LSNNO for Case $i = 3$

| r | ℓ | it | | %act |
|-----|--------|-------|-------|------|
| | | TRNNO | LSNNO | |
| 0.0 | 11 | 13 | 54 | 1.1 |
| | 12 | 13 | 58 | 1.1 |
| | 13 | 12 | 68 | 1.1 |
| | 14 | 13 | 53 | 1.1 |
| | 15 | 13 | 150 | 3.4 |
| | 16 | 14 | 76 | 1.3 |
| 0.1 | 11 | 10 | 54 | 13.1 |
| | 12 | 12 | 52 | 14.0 |
| | 13 | 9 | 48 | 14.7 |
| | 14 | 12 | 101 | 14.7 |
| | 15 | 9 | 85 | 17.9 |
| | 16 | 11 | 132 | 17.1 |
| 0.2 | 11 | 9 | 83 | 28.6 |
| | 12 | 23 | 142 | 30.8 |
| | 13 | 9 | 159 | 35.2 |
| | 14 | 11 | 237 | 40.1 |
| | 15 | 9 | | |
| | 16 | 8 | | |

TABLE 10
Comparison with LSNNO for Case $i = 3$ (higher dimensions)

| r | ℓ | it | | %act |
|-----|--------|-------|-------|------|
| | | TRNNO | LSNNO | |
| 0.0 | 19 | 12 | 142 | 1.1 |
| 0.1 | 22 | 10 | 495 | 26.0 |

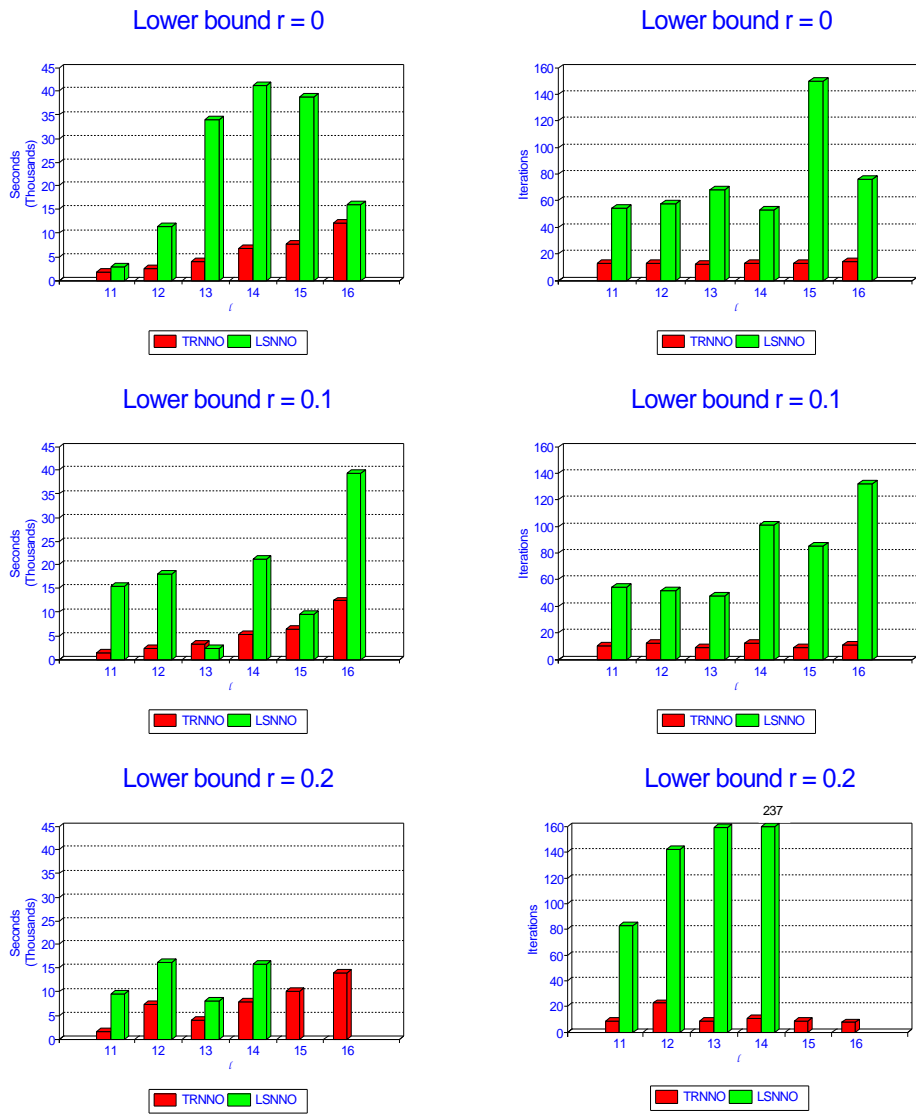


FIG. 6. Comparison with LSNN0 on cpu-times and iterations for fixed bounds (Case $i = 3$)

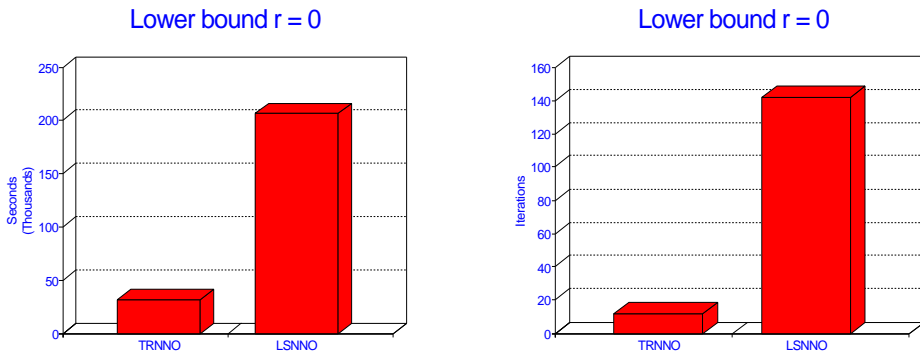


FIG. 7. Comparison with LSNN0 for $l = 19$ (Case $i = 3$)

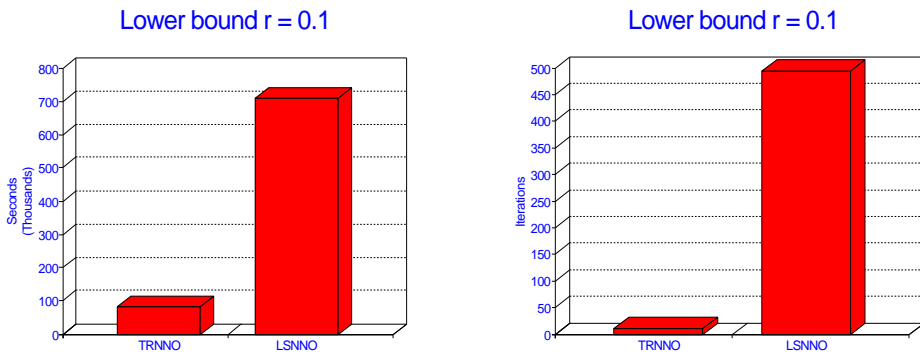


FIG. 8. Comparison with LSNN0 for $l = 22$ (Case $i = 3$)

Acknowledgments. The author wish to thank Michel Bierlaire, Andy Conn, Nick Gould, Philippe Toint and Daniel Tuyttens for their useful comments and suggestions. Daniel Tuyttens also kindly gave access to his code, his test problems and his numerical results.

REFERENCES

- [1] D. P. AHLFELD, R. S. DEMBO, J. M. MULVEY, AND S. A. ZENIOS, *Nonlinear programming on generalized networks*, ACM Transactions on Mathematical Software, 13 (1987), pp. 350–367.
- [2] G. H. BRADLEY, G. G. BROWN, AND G. W. GRAVES, *Design and implementation of large-scale transshipment algorithms*, Management Science, 24 (1977), pp. 1–34.
- [3] T. M. CARPENTER, I. J. LUSTIG, J. M. MULVEY, AND D. F. SHANNO, *Higher-order predictor-corrector interior point methods with application to quadratic objectives*, SIAM J. Optimization, 3 (1993), pp. 696–733.
- [4] A. R. CONN, N. GOULD, A. SARTENAER, AND P. L. TOINT, *Global convergence of a class of trust region algorithms for optimization using inexact projections on convex constraints*, SIAM J. Optimization, 3 (1993), pp. 164–221.
- [5] ———, *Global convergence of two augmented Lagrangian algorithms for optimization with a combination of general equality and linear constraints*, Tech. Rep. 93/01, Dept. of Mathematics, FUNDP, Namur, Belgium, 1993.
- [6] ———, *Local convergence properties of two augmented Lagrangian algorithms for optimization with a combination of general equality and linear constraints*, Tech. Rep. 93/20, Dept. of Mathematics, FUNDP, Namur, Belgium, 1993.
- [7] A. R. CONN, N. I. M. GOULD, AND P. L. TOINT, *Global convergence of a class of trust region algorithms for optimization with simple bounds*, SIAM J. on Numer. Anal., 25 (1988), pp. 433–460. Correction, same journal, 26 (1989), pp.764–767.
- [8] ———, *A globally convergent augmented Lagrangian algorithm for optimization with general constraints and simple bounds*, SIAM J. on Numer. Anal., 28 (1991), pp. 545–572.
- [9] G. B. DANTZIG, *Linear Programming and Extensions*, Princeton University Press, Princeton, USA, 1963.
- [10] R. S. DEMBO, *The performance of NLPNET, a large scale nonlinear network optimizer*, Math. Programming, Series B, 26 (1986), pp. 245–249.
- [11] ———, *A primal truncated Newton algorithm with application to large scale nonlinear network optimization*, Math. Programming, Series B, 31 (1987), pp. 43–71.
- [12] R. S. DEMBO AND J. G. KLINCEWICZ, *A scaled reduced gradient algorithm for network flow problems with convex separable costs*, Math. Programming, 15 (1981), pp. 125–147.
- [13] L. F. ESCUDERO, *A motivation for using the truncated Newton approach in a very large scale nonlinear network problem*, Mathematical Programming Studies, 26 (1986), pp. 240–245.
- [14] A. GRIEWANK AND P. L. TOINT, *On the unconstrained optimization of partially separable functions*, in Nonlinear Optimization 1981, M. J. D. Powell, ed., London and New York, 1982, Academic Press, pp. 301–312.
- [15] ———, *Partitioned variable metric updates for large structured optimization problems*, Numerische Mathematik, 39 (1982), pp. 119–137.
- [16] M. D. GRIGORIADIS, *An efficient implementation of the network simplex method*, Math. Programming, 26 (1986), pp. 83–111.
- [17] J. L. KENNINGTON AND R. V. HELGASON, *Algorithms for Network Programming*, John Wiley, New York, 1980.
- [18] J. J. MORÉ, *Recent developments in algorithms and software for trust region methods*, in Mathematical Programming: The State of the Art, A. Bachem, M. Grötschel, and B. Korte, eds., Berlin, 1983, Springer Verlag, pp. 258–287.
- [19] B. A. MURTAGH AND M. A. SAUNDERS, *Large-scale linearly constrained optimization*, Math. Programming, 14 (1978), pp. 41–72.
- [20] Y. SHEFFI, *Urban Transportation Networks*, Prentice-Hall, Englewood Cliffs, USA, 1985.
- [21] P. L. TOINT AND D. TUYTTENS, *On large scale nonlinear network optimization*, Math. Programming, Series B, 48 (1990), pp. 125–159.
- [22] ———, *LSNNO: a Fortran subroutine for solving large scale nonlinear network optimization problems*, ACM Transactions on Mathematical Software, 18 (1992), pp. 308–328.
- [23] D. TUYTTENS AND J. TEGHEM, *Théorie des matroïdes et optimisation combinatoire*, Belgian Journal of Operations Research, Statistics and Computer Science, 26 (1986), pp. 27–62.